$CD11c^+CD88^+CD317^+$ myeloid cells are critical mediators of persistent CNS autoimmunity

Navid Manouchehri[a], Rehana Z. Hussain[a], Petra D. Cravens[a], Ekaterina Esaulova[b], Maxim N. Artyomov[b], Brian T. Edelson[b], Gregory F. Wu[b,c], Anne H. Cross[c], Richard Doelger[a], Nicolas Loof[d], Todd N. Eagar[e], Thomas G. Forsthuber[f], Laurent Calvier[g,h], Joachim Herz[g,h,i,j], and Olaf Stüve[a,k,1]

[a]Department of Neurology and Neurotherapeutics, University of Texas Southwestern Medical Center, Dallas, TX 75390; [b]Department of Pathology & Immunology, Washington University School of Medicine, St. Louis, MO 63110; [c]Department of Neurology, Washington University School of Medicine, St. Louis, MO 63110; [d]The Moody Foundation Flow Cytometry Facility, Children's Research Institute, University of Texas Southwestern Medical Center, Dallas, TX 75390; [e]Department of Pathology and Genomic Medicine, Houston Methodist Hospital, Houston, TX 77030; [f]Department of Biology, University of Texas at San Antonio, San Antonio, TX 78249; [g]Department of Molecular Genetics, University of Texas Southwestern Medical Center, Dallas, TX 75390; [h]Center for Translational Neurodegeneration Research, University of Texas Southwestern Medical Center, Dallas, TX 75390; [i]Department of Neuroscience, University of Texas Southwestern Medical Center, Dallas, TX 75390; [j]Center for Neuroscience, Department of Neuroanatomy, Albert-Ludwigs University, 79085 Freiburg, Germany; and [k]Neurology Section, VA North Texas Health Care System, Dallas, TX 75216

Edited by Lawrence Steinman, Stanford University School of Medicine, Stanford, CA, and approved February 16, 2021 (received for review July 9, 2020)

Natalizumab, a humanized monoclonal antibody (mAb) against α4-integrin, reduces the number of dendritic cells (DC) in cerebral perivascular spaces in multiple sclerosis (MS). Selective deletion of α4-integrin in $CD11c^+$ cells should curtail their migration to the central nervous system (CNS) and ameliorate experimental autoimmune encephalomyelitis (EAE). We generated $CD11c.Cre^{+/-}ITGA4^{fl/fl}$ C57BL/6 mice to selectively delete α4-integrin in $CD11c^+$ cells. Active immunization and adoptive transfer EAE models were employed and compared with WT controls. Multiparameter flow cytometry was utilized to immunophenotype leukocyte subsets. Single-cell RNA sequencing was used to profile individual cells. α4-Integrin expression by $CD11c^+$ cells was significantly reduced in primary and secondary lymphoid organs in $CD11c.Cre^{+/-}ITGA4^{fl/fl}$ mice. In active EAE, a delayed disease onset was observed in $CD11c.Cre^{+/-}ITGA4^{fl/fl}$ mice, during which $CD11c^+CD88^+$ cells were sequestered in the blood. Upon clinical EAE onset, $CD11c^+CD88^+$ cells appeared in the CNS and expressed $CD317^+$. In adoptive transfer experiments, $CD11c.Cre^{+/-}ITGA4^{fl/fl}$ mice had ameliorated clinical disease phenotype associated with significantly diminished numbers of CNS $CD11c^+CD88^+CD317^+$ cells. In human cerebrospinal fluid from subjects with neuroinflammation, microglia-like cells display coincident expression of *ITGAX* (CD11c), *C5AR1* (CD88), and *BST2* (CD317). In mice, we show that only activated, but not naïve microglia expressed CD11c, CD88, and CD317. Finally, anti-CD317 treatment prior to clinical EAE substantially enhanced recovery in mice.

multiple sclerosis | EAE | myeloid cells | CD317 | biomarker

Autoimmune disorders of the central nervous system (CNS), including multiple sclerosis (MS), are thought to be mediated by aberrant adaptive immune responses against self-antigens. In experimental autoimmune encephalomyelitis (EAE), a model of MS, activated myelin-reactive $CD4^+$ T helper cells are the main drivers of disease activity (1). In active EAE, dendritic cells (DC) are professional antigen-presenting cells (APC) at the inoculation site, namely in draining lymph nodes and other secondary lymphoid organs, where they present myelin autoantigen to naïve $CD4^+$ T lymphocytes (2). Myeloid APC within the CNS are essential for the reactivation and retention of these autoreactive $CD4^+$ T cells, and for perpetuation of disease activity. Specifically, myeloid cells within cerebral perivascular spaces previously considered DC based solely on their expression of CD11c are sufficient to permit EAE (3). Myeloid APC, including DC, use α4-integrin to gain access to sites of ongoing inflammation. We previously showed that the number of DC was significantly reduced in cerebral perivascular spaces in autopsy material of an MS patient treated with natalizumab, a humanized monoclonal antibody (mAb) against α4-integrin (4). Conceivably, antagonizing or diminishing the function of α4-integrin selectively in myeloid cells should ameliorate EAE through an impaired reactivation of CNS-specific $CD4^+$ T cells and a reduction of direct inflammatory effects exerted by these cells.

To further understand the role of $CD11c^+$ cells within the CNS during $CD4^+$ T cell-mediated CNS autoimmunity, we generated and characterized $CD11c.Cre^{+/-}ITGA4^{fl/fl}$ mice, which lack α4-integrin expression in $CD11c^+$ cells. We identified $CD11c^+CD88^+CD317^+$ as mediators of persistent clinical EAE, and propagators of inflammation within the CNS.

Materials and Methods

Generation of $CD11c.Cre^{+/-}$ α4-Integrin–Deficient Mice. Female homozygote *ITGA4*-floxed ($ITGA4^{fl/fl}$) C57BL/6 mice, generated by Thalia Papayannopoulou, University of Washington, Seattle, WA (5), were crossed with commercially available $CD11c/Cre^+$ C57BL/6 males (http://jax.org; stock no: 008068) (6), and the progeny were backcrossed to generate $CD11c^{+/-}$ $ITGA4^{fl/fl}$ mice. These mice were extensively characterized (7). Each generation of mice was genotyped via genomic PCR using CD11c-specific primers. C57BL/6 WT mice

Significance

The bone marrow-derived $CD11c^+CD88^+CD317^+$ myeloid cells within the central nervous system are associated with clinical experimental autoimmune encephalomyelitis. Transcriptional analyses identify *ITGAX*- (CD11c), *C5AR1*- (CD88), and *BST2*- (CD317) expressing cells as a distinct myeloid subset in human cerebrospinal fluid. The disease-propagating effects of these cells in experimental autoimmune encephalomyelitis can be effectively antagonized using anti-CD317 monoclonal antibody therapy.

Author contributions: N.M., B.T.E., G.F.W., A.H.C., T.G.F., J.H., and O.S. designed research; N.M., R.Z.H., P.D.C., E.E., M.N.A., B.T.E., G.F.W., A.H.C., R.D., T.N.E., and L.C. performed research; N.L. and L.C. contributed new reagents/analytic tools; N.M., R.Z.H., P.D.C., E.E., M.N.A., B.T.E., G.F.W., A.H.C., R.D., N.L., T.N.E., L.C., and O.S. analyzed data; and N.M., R.Z.H., T.G.F., J.H., and O.S. wrote the paper.

Competing interest statement: O.S. serves on the editorial boards of Therapeutic Advances in Neurological Disorders. He has served on data monitoring committees for Genentech-Roche, Pfizer, and TG Therapeutics without monetary compensation. O.S. has advised EMD Serono, Celgene, Genentech, TG Therapeutics, and Genzyme. He currently receives grant support from Sanofi Genzyme and EMD Serono. G.F.W. has received honoraria for consulting for Novartis and Genentech, and received research funding from Biogen, EMD Serono, and Roche. A.H.C. has received honoraria for consulting for Biogen, Celgene, EMD Serono, Genentech, Novartis, Roche, and TG Therapeutics; she has received compensation for speaking for Genentech.

This article is a PNAS Direct Submission.

See online for related content such as Commentaries.

[1]To whom correspondence may be addressed. Email: olaf.stuve@utsouthwestern.edu.

This article contains supporting information online at https://www.pnas.org/lookup/suppl/doi:10.1073/pnas.2014492118/-/DCSupplemental.

Published March 30, 2021.

were purchased from the Jackson Laboratories. C57BL/6 WT mice were bred and maintained in a pathogen-free facility at the University of Texas Southwestern Medical Center according to guidelines provided by the National Institute of Health and our institution. Male and female mice were utilized for experiments. Specifically, all experiments were carried out exclusively either with female or male mice, and no sex-specific effects were observed. We observed no differences regarding disease scores, cellular composition, or any of the biochemical and cellular outcomes between the two sexes. The University of Texas Southwestern Institutional Animal Care and Use Committee approved all experiments and procedures.

Peptides. Mouse myelin oligodendrocyte glycoprotein peptide 35–55 (MOG_{p35-55}) (MEVGWYRSPFSRVVHLYRNGK), synthesized by Fmoc chemistry by Quality Controlled Biochemicals and CS Bio, was utilized for active immunization EAE.

Experimental Autoimmune Encephalomyelitis. To induce active EAE, experimental mice aged 8 to 12 wk were immunized subcutaneously with myelin MOG_{p35-55} (100 μg/100 μL per mouse), emulsified in an equal volume of complete Freund adjuvant (CFA) containing 4 mg/mL H37Ra *Mycobacterium tuberculosis* (Difco, BD) in each flank as described previously (8). Upon immunization and 48 h later, experimental animals received intraperitoneal injection of 200 ng PTX in 200 μL phosphate buffered saline (PBS).

For adoptive-transfer EAE, donor cells were harvested from the draining axillary and inguinal lymph nodes of female WT C57BL/6 mice 10 d after active immunization with MOG_{p35-55}, as described above, and single-cell suspensions were prepared. $CD4^+$ T cells, including MOG_{p35-55}–reactive T cells, were purified via negative selection (EasySep Mouse $CD4^+$ T cell Isolation Kit, StemCell Technologies, Lot: 18H94653). Purified $CD4^+$ T cells were cultured for 72 h with interleukin-12 (IL-12) and MOG_{p35-55}. Subsequently, cultured cells were injected to recipient mice (10×10^6 cells per mouse intraperitoneally).

For treatment experiments, mice were injected with 250 μg of a rat anti-mouse IgG2bκ anti-CD317 mAb (BioxCell, clone 927) intraperitoneally on days 7 and 8 postimmunization. The anti-CD317mAb is a blocking IgG_{2b} variant. Specifically, we administered this isotype to avoid complement fixation and Ab-mediated depletion of $CD317^+$ cells. As controls, we decided to deliver two equal volumes of vehicle (PBS) by intraperitoneal injections on days 7 and 8.

All experimental animals were observed at least twice daily and disease severity scores were recorded based on a standard EAE scoring system; briefly: 0 = no observable clinical signs, 1 = loss of tail tone or mild hind limb weakness but not both, 2 = limp tail and mild hind limb weakness, 3 = moderate hind limb weakness with or without unilateral hind limb paralysis, 4 = complete bilateral hind limb paralysis, 5 = bilateral hind limb paralysis with fore limb weakness or moribund state or death. The following cumulative interventions were performed for all experiment animals. Moist chow was provided daily once the animal reached clinical score of 3. Regular palpation of the bladder and manual assistance with urination was performed for animals with disease score of 4; animals with EAE score of 4 were kept separated from cage mates with lower scores. Persistence of disease severity at EAE score 4, for at least 72 h or observation of EAE score 5 regardless of initiation time warranted killing using carbon dioxide asphyxiation followed by cervical dislocation as the secondary physical method. In our current animal facility, and with our current EAE induction protocol, immunized mice on the C57BL/6 background typically exhibit peak disease severity after 15 d. This is followed by a persistent plateau of clinical disease severity. For this reason, we obtained biological samples from experimental animals on day 18.

Isolation of Lymph Node Cells and Splenocytes. Cells from lymph nodes and spleen were isolated by pressing through a 70-μm nylon mesh cell retainer as described previously (8–10). Cells were treated with red blood cell (RBC) lysis buffer (Sigma-Aldrich), washed twice with cold PBS, and resuspended in PBS for counting by hemocytometer.

Bone Marrow Cell Isolation. Bone marrow cells were isolated from the femurs and tibias of mice as described previously (10). Bones were crushed with a mortar and pestle. Specimens were then passed through a 70-μm nylon mesh cell retainer. Cells were treated with RBC lysis buffer (Sigma-Aldrich), washed two times with cold PBS, and resuspended in PBS for counting with hemocytometer.

Enzymatic CNS Digestion. Mice were anesthetized with 250 mg/kg intraperitoneal injection of tribromoethanol (Avertin, Sigma Aldrich) solution and perfused with PBS through the left ventricle, as described previously (8). Brains were dissected from the skull and spinal cords were flushed from the spinal column with PBS. Tissues were finely minced using a sterile scalpel and homogenized in cold PBS. We used a commercially available neural tissue dissociation kit for enzymatic dissociation following the manufacturer's protocol (Miltenyi Biotec). Specimens were subsequently washed with cold PBS; 37% Percoll PLUS (GE Healthcare) gradient was used to remove the residual myelin. The myelin-free single-cell suspensions were counted with hemocytometer.

Separation of Blood Leukocytes. Submandibular bleeding of actively immunized mice was performed on day 12 postimmunization. Approximately 400 μL of peripheral blood was collected in EDTA tubes from each mouse. The samples from $CD11c.Cre^{+/-}ITGA4^{fl/fl}$ mice and WT controls were pooled separately. The pooled samples were diluted with 1:1 ratio with PBS and slowly added on top of 100% Ficoll in a 5-mL cryotube. Ficoll gradient layering allowed to separate peripheral blood mononuclear cells (PBMC) without the need for RBC lysis. The collected cells were counted by hemocytometer.

Western Blot Analyses. Cell lysates or tissue pieces were prepared by adding protease and phosphatase inhibitor mixture in RIPA buffer and centrifuging for 10 min at 12,000 rpm to removed debris. Lysate of 15,000 FACS-sorted cells per well were loaded into each lane of a 4 to 12% Tris gel (Bio-Rad) and subjected to electrophoresis. After blotting, nitrocellulose-membranes (Bio-Rad) were blocked for 1 h (milkpowder 5% in TBS/tween 0.1 to 0.2%) and incubated with primary antibodies (Stat1, Cell Signaling ref. 14994T; P65, Cell Signaling ref. 4764S). Binding of secondary, HRP-antibodies were visualized by ECL or ECL plus chemiluminescent (Amersham). After densitometric analyses with ImageJ, optical density values were expressed as arbitrary units and normalized for protein loading, as described in the figure legends.

In Vitro PBMC Culture Studies. A total of 0.5×10^6 PBMC were plated per well in 48-well plates in culture medium consisted of Roswell Park Memorial Institute (RPMI) 1640 (Invitrogen) supplemented with L-glutamine (2 mmol/L), sodium pyruvate (1 mmol/L), nonessential amino acids (0.1 mmol/L), penicillin (100 U/mL), streptomycin (0.1 mg/mL), 2-mercaptoethanol (1 μL of stock), and 10% fetal bovine serum (FBS). Next, 10 ng/mL IL-4, and 50 ng/mL granulocyte-monocyte colony-stimulating factor (GM-CSF), with or without 20 ng/mL of interferon-γ (IFN-γ) was added to wells. The culture medium was changed every 48 h, and cells were harvested at 72 h for flow cytometry analysis.

In Vitro Cell Migration Assay. To determine the infiltrative capacity of blood $CD11c^+$ $CD88^+$ myeloid cells in response to activation by IFN-γ and expression of CD317, an in vitro Boyden chamber assay was used. This assay is modified from the methods described previously (11). In brief, the Boyden chamber (Transwell Permeable Supports, Corning) consists of two compartments separated by a polycarbonate membrane filter (6.5 mm in diameter, with 3-μm pores) coated on its upper surface with fibronectin (Corning, Discovery laboratory ware, ref#: 354008, LOT:0167009; 10 $\mu g/cm^2$). A total of 5×10^5 PBMC, collected from the blood of C57BL/6 mice 10 d postimmunization with MOG_{p35-55}, suspended in 100 μL culture medium (see above), was added to the upper chamber. Half of the chambers also received and extra treatment of 20 ng/mL IFN-γ in the upper and lower compartments. The phenotype of cells added to the upper chamber was determined by flow cytometry prior to incubation. Following incubation for 72 h at 37 °C, the contents of both upper and lower chambers were collected separately, and the $CD45^+$ and $CD45^+$ $CD11c^+$ $CD88^+$ cells were phenotyped using multiparameter flow cytometer.

Multiparameter Flow Cytometry. A total of 1×10^6 mononuclear cells suspended in PBS were stained using fixable viability dye (Zombie NIR-BioLegend Cat#: 423105/423106) or (Zombie Aqua-BioLegend, Cat#: 423101/423102), and incubated for 15 min at room temperature following manufacturer's recommendation. Cells were then washed using 2% FBS-PBS (FACs buffer) at 1,500 rpm for 5 min, followed by incubation with 1 μg Fc Block (anti-CD16/32, Tonbo Biosciences) for 15 min at 4 °C. Cells were then stained with the following antibodies: CD45 (Alexa Flour 700-BioLegend, Clone: 30-F11 or APC/Fire 750-BioLegend Clone: 13/2.3), CD11b (V450-BD Horizon, Clone: M1/70), CD19 (BV510-Biolegend, clone: 6D5), CD3 (V500-BD Horizon, clone: 500A2), CD4 (PE-BioLegend, clone: GK1.5), CD8 (APC-BD Pharmingen, clone: 53-6.7) CD11c (APC-BioLegend, clone: N418 or BV605-BioLegend, clone: N418), MHCII (BV785, BioLegend, clone: M5/114.15.2 or BV711-BioLegend, clone: M5/114,15.2), CD49d (α4-integrin; FITC, BioLegend, clone: R1-2), CD88 (PE, BioLegend, clone: 20/70), CD317 (BV421, BioLegend, clone: 927 or PercpCy5.5-BioLegend, clone: 927) CD26 (FITC, BioLegend, clone: H194-112), CD86 (BV421, BioLegend, clone: GL-1), Iba-1 (Alexa Flour 594, Santa Cruz Biotechnology, clone: 1022-5), TMEM-119 (Alexa Fluor 488, Invitrogen, clone: V3RT1G0sz), CX3CR1 (BV421, BioLegend, clone: SA011F11) for 45 min at 4 °C. Events were recorded via BD FACS LSR Fortessa (The Moody Foundation Flow Cytometry Facility, University of Texas Southwestern, Dallas, TX), equipped with Diva

acquisition software (BD Bioscience). For FACS sorting, BD FACSARIA-II SORP (The Moody Foundation Flow Cytometry Facility, University of Texas Southwestern, Dallas, TX) was utilized. Cells were gated according to morphology side scatter (SSC-A) vs. forward scatter (FSC-A). Doublets were excluded (FSC-A vs. FSC-H and SSC-A vs. SSC-H). Live cells were selected using the viability dye. The complete gating strategy is presented in *SI Appendix*, Fig. S1. Gating for FACS sorting consisted of live singlet $CD45^{hi}CD11c^{+}MHCII^{+}CD88^{+}CD317^{+}$ cells or live singlet $CD45^{int}CD11b^{+}$ cells as microglia. In each sample, a minimum of 50×10^3 live events were recorded. FlowJo software (BD Bioscience) was used for data analysis.

T Cell Proliferation Assay. To determine the capability of APCs to present $CD4^{+}$ T cells with autoantigens, flow cytometry proliferation assays using the fluorescent dye carboxyfluorescein succinimidyl ester (CFSE) were performed. Ten days after active immunization, spleens and lymph nodes from $CD11c.Cre^{+/-}ITGA4^{fl/fl}$ mice and WT controls were harvested and processed into single-cell suspensions, as described above. Splenocytes and lymphocytes were stained with CFSE and plated at 1×10^6 cells per well. The cells were then restimulated with 10 μg/mL of MOG_{p35-55} and incubated at 37 °C for 5 d. Concanavalin A (Con A) at a concentration of 2 mg/mL and media were used as controls. On day 6 the cells were collected, blocked with anti-Fc block antibody, stained with APC CD4 antibody, and acquired and analyzed by flow cytometry.

RNA Sequencing and Analysis. We analyzed our own published single-cell RNA-sequencing (scRNA-seq) data to determine the expression of specific genes among human PBMCs and cerebral spinal fluid (CSF) cells from a set of subjects with neuroinflammation (12). Briefly, this dataset includes two subjects with untreated relapsing remitting MS, one subject with anti-MOG disorder, and two subjects positive for the HIV. The data for these latter two subjects was originally derived from Farhadian et al. (13). For those subjects whose samples were collected at Washington University School of Medicine in St. Louis, all studies were approved by the Washington University in St. Louis Institutional Review Board. Using our previously employed analysis pipeline on the 23,363 PBMCs and 14,179 CSF cells combined from all subjects, we analyzed expression of *ITGAX*, *C5AR1*, and *BST2*. Expression was visualized after construction of a Uniform Manifold Approximation and Projection (UMAP) to visualize single cells in two dimensions (12).

Statistical Analysis. Groups were compared for normality using the Kolmogorov–Smirnov test. Normally distributed data were compared using unpaired two-sided Student *t* test. Holm–Sidak post hoc analysis was performed to correct in case of multiple comparisons. All statistical analyses were two-sided and a *P* value of less than 0.05 was set as the level of statistical significance. In the figures, *P* values are shown as follows: $*P = 0.05$; $**P = 0.005$; $*** P = 0.0005$; $****P = 0.00005$; $*****P = 0.000005$. Each experiment was repeated at least once. All analyses were performed with Prism 8 (Graphpad).

Results

Reduction of α4-Integrin Expression in Naïve $CD11c.Cre^{+/-}ITGA4^{fl/fl}$ Mice. We first assessed the effectiveness of Cre-Lox recombination on the expression of α4-integrin on the surface of $CD11c^{+}$ leukocytes in $CD11c.Cre^{+/-}ITGA4^{fl/fl}$ mice. The percentage of α4-integrin expressing $CD11c^{+}$ leukocytes, collected from primary and secondary lymphoid compartments of naïve WT and $CD11c.Cre^{+/-}ITGA4^{fl/fl}$ mice was assessed using ex vivo flow cytometry. When compared with naïve WT controls, naïve $CD11c.Cre^{+/-}ITGA4^{fl/fl}$ mice had a significantly lower frequency of $CD11c^{+}$ cells expressing α4-integrin in spleen (Fig. 1*A*), lymph nodes (Fig. 1*B*), bone marrow (Fig. 1*C*), and blood (Fig. 1*D*) ($P < 0.0005$). This observation confirms that Cre-mediated gene recombination diminished the expression of α4-integrin in $CD11c.Cre^{+/-}ITGA4^{fl/fl}$ mice. In order to ascertain that $CD11c.Cre^{+/-}ITGA4^{fl/fl}$ mice do not have altered absolute $CD11c^{+}$ cell numbers, we assessed the percentage of $CD11c^{+}$ cells from total viable cells in different compartments (Fig. 1 *E–H*) and compared them to controls. The percentage of $CD11c^{+}$ cells in the spleen (Fig. 1*E*) of $CD11c.Cre^{+/-}ITGA4^{fl/fl}$ mice was significantly higher than WT controls ($P < 0.05$); however, there was no difference between the two groups regarding the percentage of total $CD11c^{+}$ cells in other compartments. We also confirmed a similar α4-integrin expression by $CD11c^{+}$ leukocytes between WT and $ITGA4^{fl/fl}$ mice across multiple generations, which were found to be indistinguishable. In subsequent experiments, we only compared results between $CD11c.Cre^{+/-}ITGA4^{fl/fl}$ mice and WT controls.

Clinical Onset of Active EAE Is Delayed in $CD11c.Cre^{+/-}ITGA4^{fl/fl}$ Mice. Based on our observations in a postautopsy study of progressive multifocal leukoencephalopathy related to natalizumab therapy (4) and the critical role of DC in the initiation and perpetuation of CNS autoimmunity, we hypothesized that limited expression of α4-integrin by $CD11c^{+}$ cells would lead to reduction of severity of clinical EAE scores. Active EAE was induced in $CD11c.Cre^{+/-}ITGA4^{fl/fl}$ mice and WT controls by immunization with MOG_{p35-55} in CFA. There was no significant difference between $CD11c.Cre^{+/-}ITGA4^{fl/fl}$ mice and WT controls regarding disease severity following active immunization (Fig. 2*A*). However, the onset of clinical EAE was significantly and reproducibly delayed by at least 1 d in $CD11c.Cre^{+/-}ITGA4^{fl/fl}$ mice as compared with WT controls (Fig. 2*B*). Going forward, we will refer to the delay in disease onset as "EAE onset lag." Moreover, we will refer to an EAE phenotype that continues beyond a brief monophasic clinical episode as "persistent clinical EAE." The EAE onset lag allowed us to characterize cellular events in relevant tissues during the preclinical stage and the early onset of EAE in $CD11c.Cre^{+/-}ITGA4^{fl/fl}$ mice in comparison to WT controls, and characterize the contribution of immune cell subsets. Ex vivo flow cytometry analyses of the peripheral lymphoid tissues and CNS compartment during acute and ongoing EAE stages were performed.

Antigen Presentation Is Intact in $CD11c.Cre^{+/-}ITGA4^{fl/fl}$ Mice. Previous studies indicated that blocking very late-activating antigen 4 (VLA-4; α4β1-integrin) with mAb negatively impacted the ability of $CD4^{+}$ T cells to proliferate, perhaps suggesting a role for α4-integrin as a costimulatory molecule (14, 15). We assessed this in $CD11c.Cre^{+/-}ITGA4^{fl/fl}$ mice and WT controls through flow cytometry-based recall proliferation assays. MOG_{p35-55}–specific $CD4^{+}$ T cells were cocultured with different ratios of $CD11c^{+}$ APC harvested from $CD11c.Cre^{+/-}ITGA4^{fl/fl}$ mice and WT controls. Ex vivo flow cytometry assessment of the $CD4^{+}$ T cells proliferation based on CFSE dilution indicated that there was no significant difference between $CD11c.Cre^{+/-}ITGA4^{fl/fl}$ mice and WT controls regarding the recall response by the $CD4^{+}$ T cells (Fig. 2*C*). This suggested that antigen (Ag) presentation and T cell activation remained intact in $CD11c.Cre^{+/-}ITGA4^{fl/fl}$ mice, despite a significantly lower expression of α4-integrin by APC.

Leukocyte Composition aside from the CD11c Cell Lineage Is Unaltered in $CD11c.Cre^{+/-}ITGA4^{fl/fl}$ Mice. Next, we investigated whether the delayed onset of clinical EAE in $CD11c.Cre^{+/-}ITGA4^{fl/fl}$ mice was accompanied by an altered composition of leukocytes in different compartments. Flow cytometry analysis of immune cell populations revealed that leukocyte subtypes including $CD45^{+}$, $CD19^{+}$, $CD4^{+}$, and $CD8^{+}$ cells, from $CD11c.Cre^{+/-}ITGA4^{fl/fl}$ mice and WT controls, had similar composition in different compartments during naïve states as well as during acute and persistent clinical EAE (*SI Appendix*, Fig. S2). Few $CD45^{hi}$ cells were detectable within naïve CNS tissues from both $CD11c.Cre^{+/-}ITGA4^{fl/fl}$ mice and WT controls, while $CD45^{int}$ cells were present in both (*SI Appendix*, Fig. S3*A*); following the onset of clinical EAE in both groups, $CD45^{hi}$ cells were abundantly present inside the CNS compartment (*SI Appendix*, Fig. S3*B*). These observations suggest that the observed EAE onset lag was not driven by impaired access of immune cell outside the $CD11c^{+}$ lineage to the CNS compartment.

$CD11c^{+}$ Cells Sequester in Peripheral Blood Prior to the Onset of Clinical Active EAE. As shown earlier, we observed that the onset of clinical EAE following active immunization was consistently delayed in

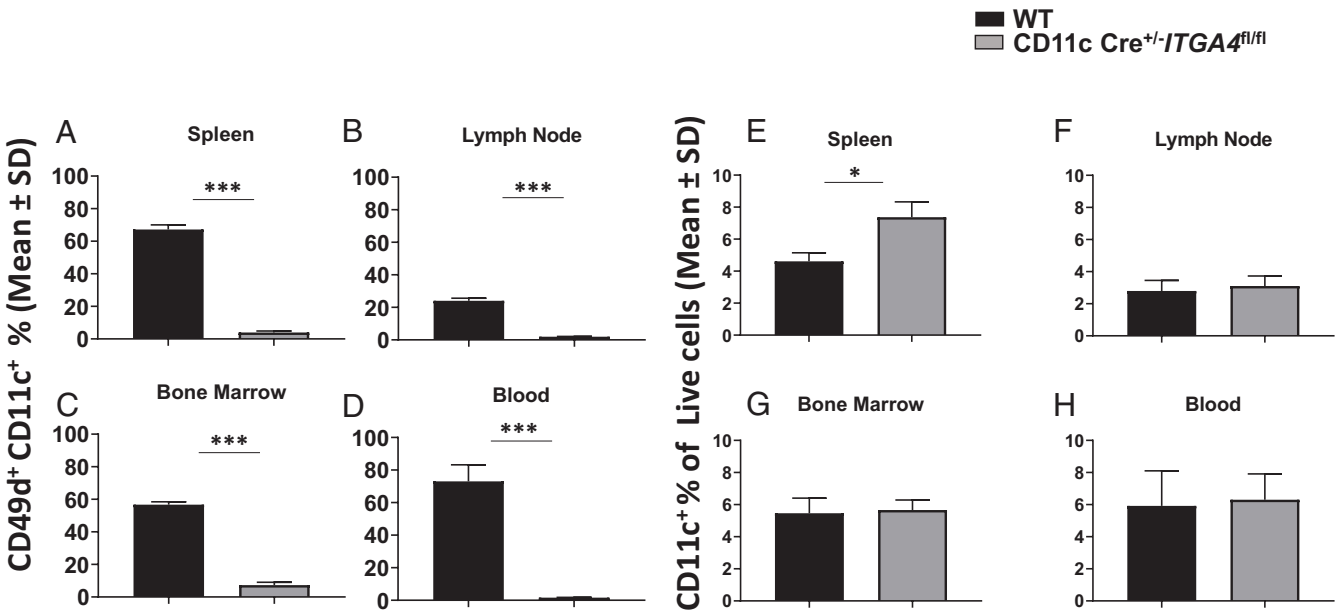

Fig. 1. CD11c.Cre$^{+/-}$*ITGA4*$^{fl/fl}$ mice exhibited reduced expression of α4-integrin by CD11c$^+$ cells. The mean ± SD of α4-integrin (CD49d)-expressing CD11c$^+$ cells (%) from total 50 × 10^3 recorded viable cells in (*A*) spleen, (*B*) lymph node, (*C*) bone marrow, and (*D*) blood of naïve WT and CD11c.Cre$^{+/-}$*ITGA4*$^{fl/fl}$ mice is shown (n = 9 experimental animals per group; data show the pooled analysis of all study cohorts). The α4-integrin expression in CD11c.Cre$^{+/-}$*ITGA4*$^{fl/fl}$ mice compared to C57BL/6 WT controls is significantly reduced in all compartments (***$P < 0.0005$). The absolute number as a percentage of CD11c$^+$ cells from total viable cells is not reduced in CD11c.Cre$^{+/-}$*ITGA4*$^{fl/fl}$ mice. The mean ± SD of CD11c$^+$ cells (%) from total 50 × 10^3 recorded viable cells in (*E*) spleen, (*F*) lymph node, (*G*) bone marrow, and (*H*) blood is shown (n = 9 experimental animals per group; data show the pooled analysis of all study cohorts). The percentage of CD11c$^+$ cells was significantly higher in the spleen among CD11c.Cre$^{+/-}$*ITGA4*$^{fl/fl}$ mice (*$P < 0.05$). There was no difference between the two groups regarding the percentage of CD11c$^+$ cells in other compartments.

the CD11c.Cre$^{+/-}$*ITGA4*$^{fl/fl}$ group. The EAE onset lag provided a window for studying the composition of the inflammatory milieu in different compartments. Using ex vivo flow cytometry, we compared the percentage of live CD45$^+$MHCII$^+$CD11c$^+$ cells collected from the peripheral blood and CNS (brain and spinal cord) of CD11c.Cre$^{+/-}$*ITGA4*$^{fl/fl}$ mice and WT controls at two time points following induction of active EAE. The cells were collected from both groups upon the onset of clinical EAE among the WT controls on day 11 postimmunization (Fig. 2*D*). In this setting, CD11c$^+$ cells were significantly more frequent in the blood of CD11c.Cre$^{+/-}$*ITGA4*$^{fl/fl}$ mice compared to WT controls (Fig. 2*E*) ($P < 0.00005$); simultaneously, these cells were significantly more abundant in the brain (Fig. 2*F*) and spinal cord (Fig. 2*G*) of the WT controls ($P < 0.005$). Subsequently, cells were collected from mice in both groups at the onset of clinical EAE among the CD11c.Cre$^{+/-}$*ITGA4*$^{fl/fl}$ mice on day 14 postimmunization (Fig. 2*H*). There were no significant differences between the frequencies of CD11c$^+$ cells inside the peripheral circulation (Fig. 2*I*), brain (Fig. 2*J*), and spinal cord (Fig. 2*K*) of the CD11c.Cre$^{+/-}$*ITGA4*$^{fl/fl}$ mice compared to WT controls. Taken together, these findings indicate that the clinical onset of EAE is closely related to the increased appearance of CD11c$^+$ cells inside the CNS compartment. The concomitant disappearance of these cells from the blood suggests that CD11c$^+$ cells inside the CNS originated from cells entering from the peripheral compartment.

CD11c$^+$ Cells and CD11c$^+$CD88$^+$ Cells Distribute Similarly Among Tissues during Active EAE. We observed that the onset of clinical EAE was preceded by the accumulation of CD11c$^+$ cells in the blood, and their subsequent appearance inside the CNS was associated with the onset of clinical disease. Next, we wanted to further characterize immunologic traits of these cells. Bone marrow-derived CD11c$^+$ myeloid cells in the blood are comprised to a significant extent of CD88$^+$ monocyte-derived cells (16–18). Using ex vivo flow cytometry, we assessed the percentage of CD88 expressing CD11c$^+$ cells collected from the blood and CNS of CD11c.Cre$^{+/-}$*ITGA4*$^{fl/fl}$ mice and WT controls. In both groups, the majority of CD11c$^+$ cells in the blood and CNS also expressed CD88. At the time of the onset of clinical EAE in the WT control group (Fig. 2*D*) (day 11 postimmunization), CD11c$^+$ CD88$^+$ cells accumulated in the blood of CD11c.Cre$^{+/-}$*ITGA4*$^{fl/fl}$ mice (Fig. 2*L*) ($P < 0.00005$), while they were significantly more frequent inside the brain (Fig. 2*M*) and spinal cord (Fig. 2*N*) of WT controls ($P < 0.005$). Subsequently, following the onset of clinical EAE in CD11c.Cre$^{+/-}$*ITGA4*$^{fl/fl}$ mice (Fig. 2*H*) (day 14 postimmunization), the percentage of CD11c$^+$ CD88$^+$ cells in the blood was diminished (Fig. 2*O*), while it was increased in the brain (Fig. 2*P*) and spinal cord (Fig. 2*Q*). At that time, there were no differences between the two experimental groups in any of these compartments.

CD11c$^+$CD88$^+$ Cells Express CD317 inside the CNS but Not in Blood. We observed that CD11c$^+$ cells from CD11c.Cre$^{+/-}$*ITGA4*$^{fl/fl}$ mice were initially delayed from gaining access to the CNS, but ultimately accumulated inside the brain and spinal cord of CD11c.Cre$^{+/-}$*ITGA4*$^{fl/fl}$ mice (Fig. 2). This suggested redundancy in adhesion molecules by CD11c$^+$ myeloid cells. CD317 is a lipid raft-associated glycosyl-phosphatidylinositol (gpi)-anchored protein that is constitutively expressed by plasmacytoid DC, mature B cells, plasma cells, and other leukocytes (19, 20). More recently, CD317 has also been shown to function as an adhesion molecule for myeloid cells (21). To determine whether CD317 is up-regulated by CD11c$^+$CD88$^+$ cells upon entry into the CNS and serves as an adhesion molecule, we assessed its expression by CD11c$^+$ cells in our model. During active EAE, we found that CD317-expressing CD11c$^+$CD88$^+$ cells in the peripheral circulation were significantly less frequent ($P < 0.0005$) than CD11c$^+$CD88$^+$CD317$^-$ cells (Fig. 3*A*). In contrast, the percentage of CD11c$^+$CD88$^+$ cells expressing CD317 was significantly higher than the percentage of

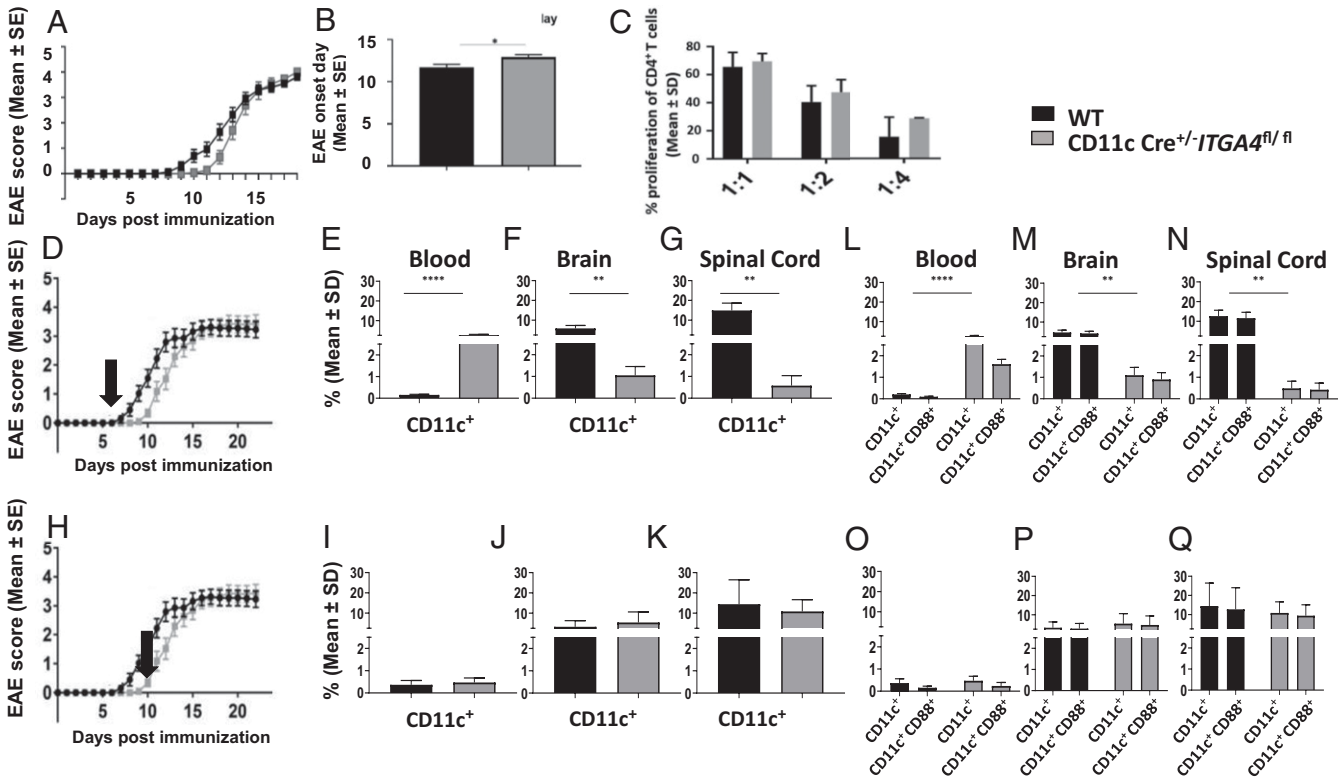

Fig. 2. The onset of active EAE is consistently delayed among the CD11c.Cre$^{+/-}$*ITGA4*$^{fl/fl}$ mice. (*A*) The mean ± SE of clinical EAE following active immunization are presented ($n = 24$ experimental animals per group; data display pooled analysis of all study cohorts). (*A* and *B*) The onset of disease was significantly delayed in the CD11c.Cre$^{+/-}$*ITGA4*$^{fl/fl}$ group ($*P < 0.05$). (*C*) The percentage (mean ± SD) of proliferating Ag-specific CD4$^+$ T cells cocultured with different dilutions of CD11c$^+$ splenocytes from CD11c.Cre$^{+/-}$*ITGA4*$^{fl/fl}$ mice and WT controls is shown. There was no significant difference between the two groups. Clinical EAE is preceded by accumulation of CD11c$^+$ cells in peripheral blood. The mean ± SD of percentage of CD11c$^+$ and CD11c$^+$CD88$^+$ cells from total 50×10^3 recorded viable cells upon the onset of actively induced clinical EAE in (*D*) C57BL/6 WT controls (day 11 postimmunization), in (*E* and *L*) blood, (*F* and *M*) brain, and (*G* and *N*) spinal cord, and after the onset of clinical EAE in CD11c.Cre$^{+/-}$*ITGA4*$^{fl/fl}$ mice (*H*) in (*I* and *O*) blood, (*J* and *P*) brain, and (*K* and *Q*) spinal cord and is shown ($n = 8$ experimental animals per group; data show pooled analysis of all study cohorts). (*E* and *I*) There was a significant sequestration of CD11c$^+$ and CD11c$^+$CD88$^+$cells in the blood of CD11c.Cre$^{+/-}$*ITGA4*$^{fl/fl}$ compared to controls upon the onset of clinical EAE ($****P < 0.00005$), while CD11c$^+$ cells were significantly more frequent in the (*F* and *J*) brain and (*G* and *K*) spinal cord of WT mice ($**P = 0.005$). (*F*–*H*) There was no difference between the two groups in any of the compartments after the start of the clinical EAE among the CD11c.Cre$^{+/-}$*ITGA4*$^{fl/fl}$ mice (day 14 postimmunization; $P > 0.05$).

CD11c$^+$ CD88$^+$ cells not expressing CD317 in the brain (Fig. 3*B*) and spinal cord (Fig. 3*C*) ($P < 0.0005$). Together, these observations suggest that CD11c$^+$CD88$^+$ cells in the peripheral circulation start expressing CD317 upon entry into the CNS compartment at the onset of clinical EAE.

The expression of CD317 is inducible through engagement of signal transducer and activator of transcription (STAT) following exposure to type I or type II IFN (22–24). To investigate whether CNS CD11c$^+$CD88$^+$CD317$^+$ cells originate from blood CD11c$^+$CD88$^+$ cells at the onset of clinical EAE, we collected PBMC from WT mice immunized with MOG_{p35-55}, prior to the expected onset of clinical EAE (day 10 postimmunization). In vitro culture was performed with or without stimulation with IFN-γ. Subsequent flow cytometry analysis of the cultured cells revealed that CD11c$^+$CD88$^+$ cells that were exposed to IFN-γ in culture up-regulated CD317 on their cell surface (Fig. 3*D*). The percentage of CD11c$^+$CD88$^+$CD317$^+$ was significantly higher in the IFN-γ–treated group ($P < 0.0005$). Interestingly, the fraction of CD11c$^+$CD88$^+$ cells expressing CD317 after in vitro exposure to IFN-γ was comparable to that of these cells observed in the CNS compartment during clinical EAE in both experimental groups, and significantly higher than that of blood CD11c$^+$CD88$^+$ cells (Fig. 3*E*).

IFN-γ Promotes the Migration of CD11c$^+$CD88$^+$CD317$^+$ across Biological Barriers. Once it was established that IFN-γ mediates the expression of CD317 in blood CD11c$^+$CD88$^+$ cells, we aimed to assess whether IFN-γ impacts migration capacity. PBMC from C57BL/6 WT mice immunized with MOG_{p35-55} were collected and inserted into the upper compartment of a Boyden chamber with or without IFN-γ. We were able to show that IFN-γ significantly enhanced the number of CD11c$^+$CD88$^+$CD317$^+$ cells that migrated to the bottom chamber after 72 h (Fig. 3*F*).

Proinflammatory Signaling Pathways Are Activated in CD11c$^+$CD88$^+$CD317$^+$ Cells. Our previous observation suggests a proinflammatory role for CD11c$^+$CD88$^+$CD317$^+$ cells in EAE. Using Western blot analyses, we assessed the expression of proinflammatory STAT-1 and NF-κB transcription factors among these cells and compared them to that of the CNS microglia of these mice during acute EAE (day 14 postimmunization) as well as naïve microglia. We were able to show that compared to naïve and postacute EAE microglia, CD11c$^+$CD88$^+$CD317$^+$ cells expressed significantly higher levels of STAT-1 (Fig. 3*G*) and NF-κB (Fig. 3*H*) ($P < 0.0005$ and $P < 0.005$, respectively). While microglia collected from the CNS of acute EAE mice expressed significantly higher levels of STAT-1 compared to naïve microglia (Fig. 3*G*) ($P < 0.0005$), there was no difference regarding the expression NF-κB (Fig. 3*H*).

CD11c$^+$CD88$^+$ Cells and CD11c$^+$CD88$^+$CD317$^+$ Cells Express CD11b. To characterize blood CD11c$^+$CD88$^+$ cells during preclinical EAE as well as CNS CD11c$^+$CD88$^+$CD317$^+$ cells during established EAE, we assessed both cell types for CD11b expression. CD11b

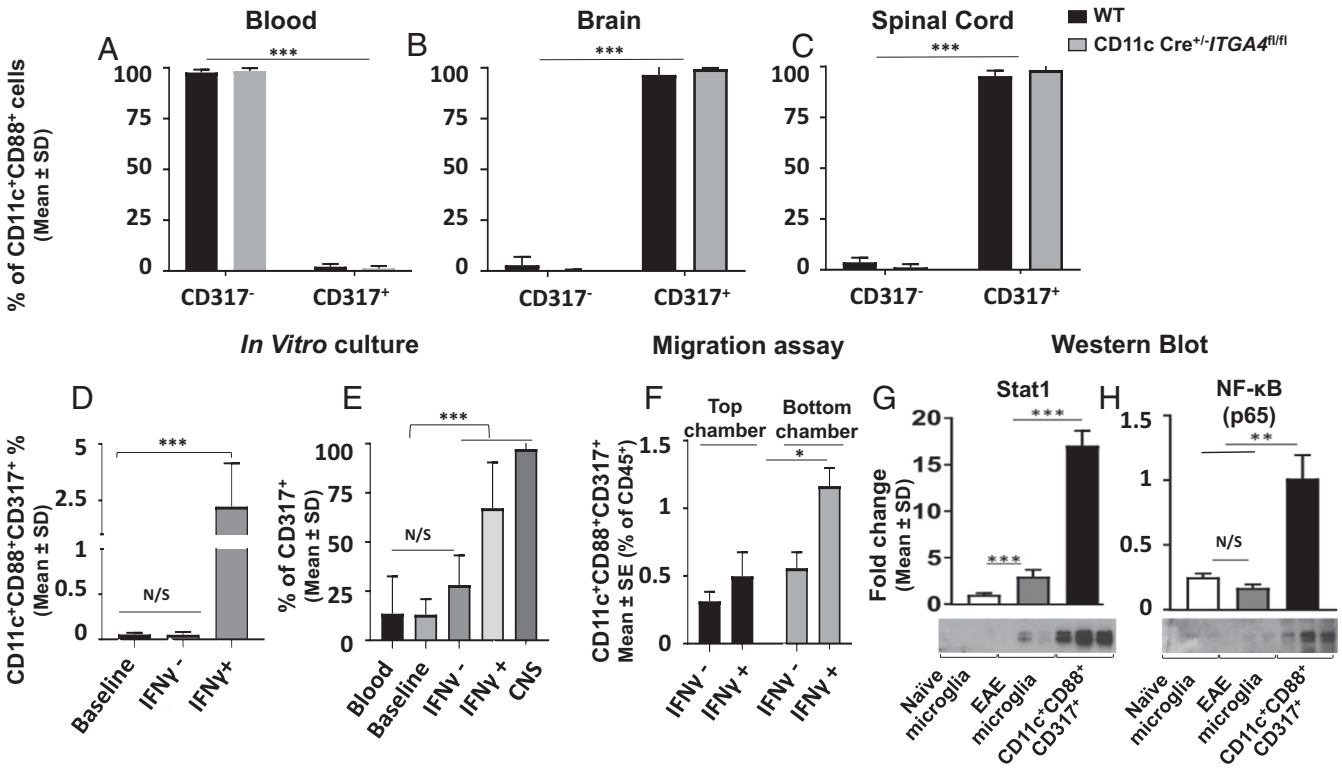

Fig. 3. CD11c$^+$CD88$^+$ cells start expressing CD317 inside the CNS compartment at the onset of active clinical EAE. The mean ± SD of the percentage of CD11c$^+$CD88$^+$ cells that express CD317 in (*A*) blood, (*B*) brain, and (*C*) spinal cord during actively induced EAE in CD11c.Cre$^{+/-}$*ITGA4*$^{fl/fl}$ mice or C57BL/6 WT controls is shown (n = 8 experimental animals per group; data show pooled analysis of all study cohorts). CD11c$^+$CD88$^+$ cells in the (*A*) blood are mostly CD317$^-$, while inside the (*B* and *C*) brain and spinal cord CD317$^+$ cells constitute the majority of the CD11c$^+$CD88$^+$ cells (***$P < 0.0005$). (*D*) The mean ± SD of CD11c$^+$ CD88$^+$CD317$^+$ cells following in vitro culture (n =12 replicates per group; data show pooled analysis of all study cohorts). (*D*) IFN-γ significantly up-regulates the expression of CD317 in CD11c$^+$CD88$^+$ cells (***$P < 0.0005$). (*E*) The mean ± SD of percentage of CD317$^+$ cells of all CD11c$^+$CD88$^+$ cells is shown, and approaches the percentage of CD317$^+$ cells of all CD11c$^+$CD88$^+$ cells within the CNS of mice with clinical EAE. (*F*) IFN-γ enhances the migratory capability of CD11c$^+$CD88$^+$CD317$^+$ cells. There was a significant increase in the percentage of CD11c$^+$CD88$^+$CD317$^+$ cells from total CD45$^+$ cells in the bottom chamber in the presence of IFN-γ (*$P = 0.05$; $n = 4$ replicates per group are shown). (*G*) CD11c$^+$CD88$^+$CD317$^+$ cells inside the CNS compartment express high levels of STAT-1 and NF-κB (p65) transcription factors. The mean ± SD of fold-change among CD11c$^+$CD88$^+$CD317$^+$ cells for STAT-1 (*G*) and NF-κB (p65) (*H*) expression were significantly higher compared to both naïve microglia and active EAE microglia (day 14 postimmunization) (***$P < 0.0005$ and **$P < 0.005$, respectively). The mean ± SD of fold-change in STAT-1 was also significantly higher among the active EAE microglia compared to naïve microglia (*G*) (***$P < 0.0005$). All Western blot experiments were conducted as triplicates.

is expressed on granulocyte, macrophages, monocytes, and natural killer cells (25). We observed that CD11c$^+$CD88$^+$ cells and CD11c$^+$CD88$^+$CD317$^+$ cells also express CD11b (*SI Appendix*, Fig. S1), a property that has been assigned to migratory DC (25).

Decreased EAE Severity in the Absence of CD11c$^+$CD88$^+$CD317$^+$ Cells in the CNS. In active EAE, the microenvironment outside of the CNS in this EAE model is defined by an excess of IFN-γ (26). In contrast, the adoptive transfer of myelin-reactive CD4$^+$ T cells, many of which are Th1 cells, creates an IFN-γ–rich environment inside the CNS, but not in other tissues (27–29). MOG_{p35-55}–reactive CD4$^+$ T cells from WT donors were transferred to CD11c.Cre$^{+/-}$*ITGA4*$^{fl/fl}$ and WT control recipients (Fig. 4*A*). Analysis of clinical disease scores in both groups longitudinally revealed a striking reduction of clinical disease in the CD11c.Cre$^{+/-}$*ITGA4*$^{fl/fl}$ mice as compared with WT controls ($P < 0.0005$) (Fig. 4*A*). Specifically, the disease course was substantially ameliorated and abbreviated, and devoid of the persistent clinical phase that is routinely expected in the C57BL/6 model of EAE. Ex vivo flow cytometry revealed that CD11c$^+$CD88$^+$ cells were significantly more frequent in the blood of CD11c.Cre$^{+/-}$*ITGA4*$^{fl/fl}$ mice compared to WT controls at day 18 postadoptive transfer (Fig. 4*B*) ($P < 0.005$). Further ex vivo flow cytometry-based characterization of immune cells in the peripheral compartment and CNS of mice in both groups indicated that CD11c.Cre$^{+/-}$*ITGA4*$^{fl/fl}$ mice that showed less severe disease course also exhibited significantly lower percentage of CD11c$^+$ cells, CD11c$^+$CD88$^+$ cells, and CD11c$^+$CD88$^+$CD317$^+$ cells inside the brain (Fig. 4 *C* and *F*) and spinal cord (Fig. 4 *D* and *G*) ($P < 0.005$). Interestingly, CD11c$^+$CD88$^+$CD317$^+$ were extremely rare in the blood of both CD11c.Cre$^{+/-}$*ITGA4*$^{fl/fl}$ mice and WT controls (Fig. 4*E*). In summary, these observations suggest an association between the presence of CD11c$^+$CD88$^+$CD317$^+$ cells inside the CNS and the severity of acute EAE, as well as the transition to persistent clinical EAE.

Coincident Expression of *ITGAX*, *C5AR1*, and *BST2* by Human CSF Microglia-like Cells in Neuroinflammation. After identifying the association of CD11c$^+$CD88$^+$CD317$^+$ cells with EAE disease severity, we aimed to determine whether this cell type could also be identified in human tissues relevant to CNS autoimmunity. Using scRNA-seq, our group previously described 20 clusters representing distinct cell populations within PBMCs and CSF of subjects with neurologic diseases (Fig. 5*A*) (12). Our report, as well as recent reports from other groups (30–32), has described a distinct cell type within the CSF displaying the gene-expression profile of microglia (30, 33, 34). We examined our published dataset for the individual expression of *BST2*, *C5AR1*, and *ITGAX*, the human genes encoding CD317, CD88, and CD11c (Fig. 5 *B* and *C*).

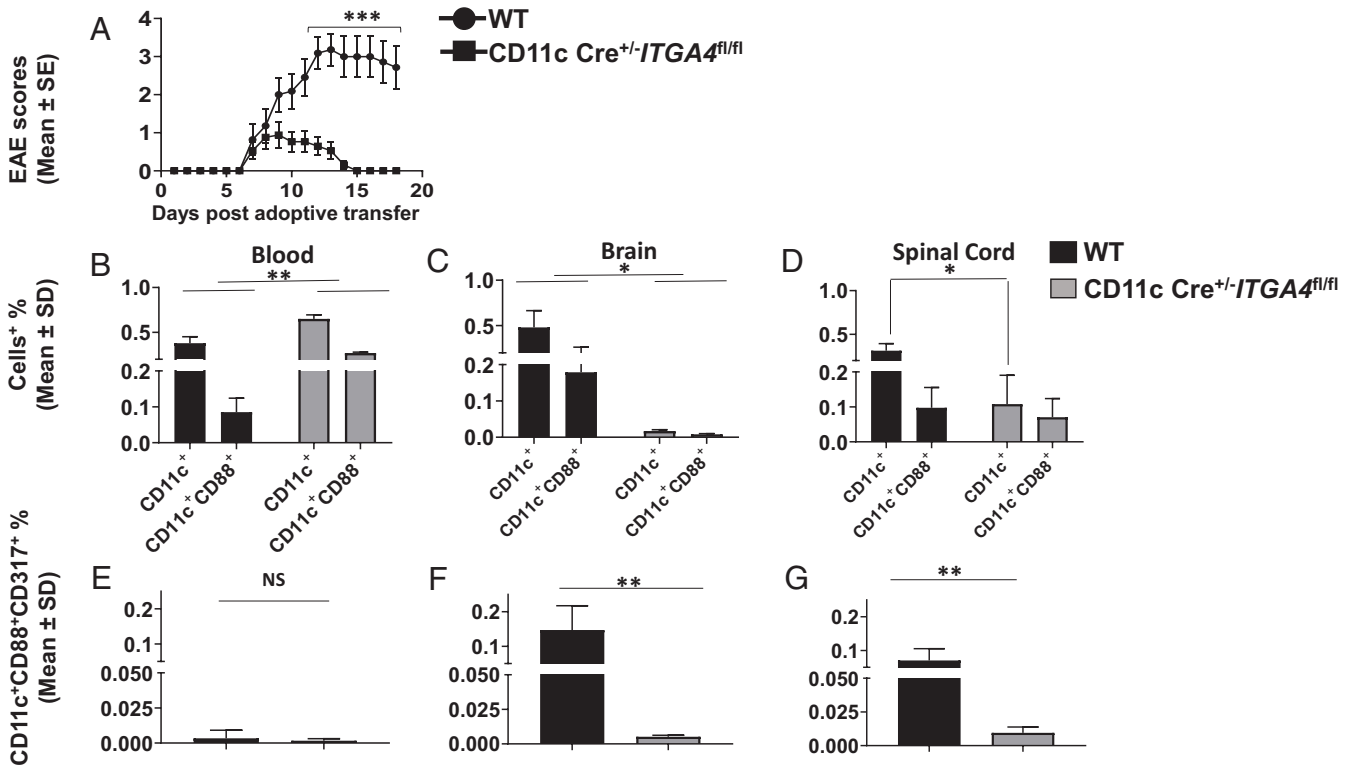

Fig. 4. Adoptive transfer of MOG_{p35-55}–specific $CD4^+$ T cells into CD11c.$Cre^{+/-}$ITGA4$^{fl/fl}$ mice causes ameliorated EAE. (*A*) Adoptive transfer EAE was induced by transferring MOG_{p35-55}–reactive $CD4^+$ T cells from C57BL/6 WT mice into CD11c.$Cre^{+/-}$*ITGA4*$^{fl/fl}$ mice or C57BL/6 WT controls. The mean ± SE of clinical EAE scores following adoptive transfer are presented ($n = 11$ experimental animals per group; data show pooled analysis of all study cohorts). Clinical disease among the CD11c.$Cre^{+/-}$*ITGA4*$^{fl/fl}$ was significantly ameliorated (***$P < 0.0005$). The percentages of $CD11c^+$ cells, $CD11c^+CD88^+$ cells (mean ± SD) of 50×10^3 recorded viable cells in (*B*) blood, (*C*) brain, and (*D*) spinal cord during clinically persistent EAE in the WT are shown ($n = 3$ experimental animals per group; data show pooled analysis of all study cohorts). The percentage of $CD11c^+CD88^+CD317^+$ cells (mean ± SD) of 50×10^3 recorded viable cells is also shown in (*E*) blood, (*F*) brain, and (*G*) spinal cord. There was a significant reduction of the (*C* and *D*) $CD11c^+CD88^+$ and (*F* and *G*) $CD317^+$ cells in the CNS of CD11c.$Cre^{+/-}$*ITGA4*$^{fl/fl}$ compared to WT controls (*$P < 0.05$). $CD11c^+$ $CD88^+$ cells were significantly more frequent in the (*A*) blood of CD11c.$Cre^{+/-}$*ITGA4*$^{fl/fl}$ mice compared to WT controls (**$P < 0.005$; NS, not significant) ($n = 3$ experimental animals per group; data show pooled analysis of all study cohorts).

The collective expression of these three genes was concentrated within myeloid cell populations, most notably within CSF microglia-like cells (Fig. 5*D*). These data suggest that a microglia-like population of cells within human CSF that expresses this combination of genes is relevant to neuroinflammation.

Activated, but Not Naïve, Microglia Express CD11c, CD88, and CD317. Intrigued by the finding that expression of *ITGAX*, *C5AR1*, and *BST2* localize within human CSF microglia-like cells by transcriptomic analyses, we aimed to determine whether parenchymal microglia also express these surface markers. Due to the lack of human CNS tissue, we decided to assess murine microglia cells. Microglia were defined as viable CD45 intermediate (int), $CD11b^+$ cells (Fig. 6*A*). Microglia from naïve mice did not express CD88 and CD317 concomitantly (Fig. 6*B*). Moreover, naïve microglia are not high expressers of MHC II and CD11c (Fig. 6*C*). In contrast, microglia from mice with established active EAE express high levels of CD88 and CD317 (Fig. 6 *D* and *F*), as well as MHC II and CD11c (Fig. 6 *E* and *G*). In summary, these data indicate that CNS $CD11c^+CD88^+CD317^+$ cells associated with CNS autoimmune disease resemble activated parenchymal microglia. We further assessed $CD45^{int}$ $CD11b^+CD11c^+CD88^+CD317^+$ cells defined as microglia, and $CD45^{hi}$ $CD11c^+CD88^+CD317^+$ cells defined as bone marrow-derived myeloid cells through ex vivo flow cytometry (*SI Appendix*, Fig. S3). First, $CX3CR1^+$ cells from $CD45^{int}$ $CD11c^+CD88^+CD317^+$and $CD45^{hi}$ $CD11c^+CD88^+CD317^+$ cells were gated for (*SI Appendix*, Fig. S3*E*). Microglia were further defined as $CX3CR1^+$TMEM-119^+Iba-1^+ (*SI Appendix*, Fig. S3 *F* and *G*), while nonmicroglia were further defined as $CX3CR1^+$TMEM-119^-Iba-1^- (*SI Appendix*, Fig. S3 *J* and *K*). In naïve mice and during different stages of EAE, microglia were mostly localized within the $CD45^{int}$ gate (*SI Appendix*, Fig. S3 *H* and *R*), while nonmicroglia were situated within the $CD45^{hi}$ gate (*SI Appendix*, Fig. S3 *L* and *S*). Fewer $CD45^{int}$ microglia expressed surface CD86 (*SI Appendix*, Fig. S3*I*) compared to $CD45^{hi}$ nonmicroglia (*SI Appendix*, Fig. S3*M*).

Anti-CD317 Treatment Ameliorates EAE and Shortens Disease Duration. To provide further evidence that $CD11c^+CD88^+CD317^+$ cells are critical for establishment of persistent clinical EAE, and are therefore potential therapeutic targets, we administered a commercially available anti-CD317 rat anti-mouse IgG2b mAb on days 7 and 8 postactive immunization (Fig. 7*A*). Anti-CD317 treatment ameliorated acute EAE, with complete resolution of clinical disease. Anti-CD317 therapy resulted in an increase of $CD11c^+$, $CD11c^+CD88^+$, and $CD11c^+CD88^+CD317^+$cells in blood (Fig. 7*B*). However, the difference in cell numbers compared to vehicle controls group was not statistically significant. Furthermore, in the treatment group, $CD11c^+$, $CD11c^+CD88^+$, and $CD11c^+CD88^+CD317^+$cells in the brain (Fig. 7*C*) and spinal cord (Fig. 7*D*) were reduced compared with controls. This was statistically significant in the spinal cord (Fig. 7*D*) ($P < 0.005$). Differences in the percentages of $CD11c^+$ cells and $CD11c^+CD88^+$ in the blood, brain, and spinal cord in the anti-CD317 treatment group were driven by changes in the percentages of $CD11c^+CD88^+CD317^+$cells. Our observations suggest that anti-CD317 therapy in EAE diminishes the ability of $CD11c^+CD88^+CD317^+$ cells to

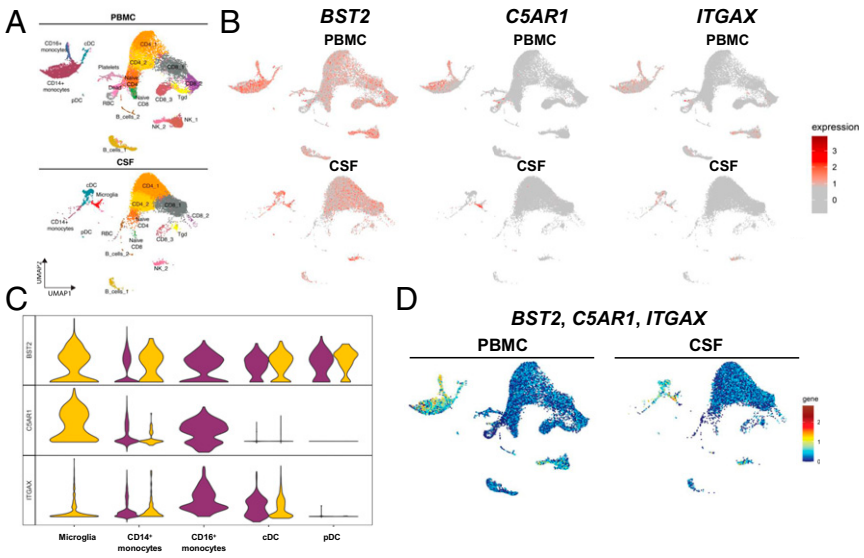

Fig. 5. Coincident expression of *ITGAX*, *C5AR1*, and *BST2* by human CSF microglia-like cells in neuroinflammation. Using scRNA-seq, our group previously described 20 clusters representing distinct cell populations in PBMC and CSF. Reprinted with permission from ref. 12. (*A*) UMAP showing cell clusters in PBMC and CSF. (*B*) Expression of *BST2*, *C5AR1*, and *ITGAX* within the UMAP of PBMC and CSF cells. (*C*) Violin plots showing expression of the indicated genes in blood (purple) and CSF (yellow) myeloid cell populations. (*D*) Coincident expression of the indicated genes within the UMAP of PBMC and CSF cells. cDC, classic dendritic cells; pDC, plasmacytoid dendritic cells.

gain access to the CNS, reducing the severity of acute EAE and the transition to persistent clinical EAE.

Discussion

In the present study, we investigated the effects of selective α4-integrin deletion in $CD11c^+$ cells in the EAE model of MS. Our observations indicate that the appearance of $CD11c^+CD88^+CD317^+$ myeloid cells inside the CNS compartment is required for establishment of persistent clinical EAE after active immunization. This is further supported by the fact that reducing the ability of these cells to gain access to the CNS via a blocking anti-CD317 mAb also prevented persistent clinical EAE. This suggests CD317 as a promising molecular target for treatment in patients with MS and related disorders.

Classically, $CD11c^+$ myeloid cells are believed to participate in processing and presentation of antigens to Ag-specific T cells during CNS autoimmunity in secondary lymphoid organs and the brain and spinal cord (2). Based on our results, we suggest that the role of $CD11c^+CD88^+CD317^+$ cells in EAE pathogenesis may be largely independent of antigen presentation. $CD88^+$ DC were previously shown to have minimal antigen presentation capability during active EAE as evidenced by a limited ability to induce T cell proliferation to recall antigens (18). In fact, initiation of clinical EAE, which requires Ag processing and presentation in peripheral lymphatic tissues, is mainly driven by classic tissue-resident classic DC, characterized by their expression of CD26 (18). We showed in our model that Ag presentation and ability to induce T cell proliferation was maintained despite the deletion of α4-integrin in CD11c cells in $Cre^{+/-}ITGA4^{fl/fl}$ mice. Furthermore, our results indicate that the pathogenic role of $CD11c^+CD88^+CD317^+$ cells in EAE appears dependent on their physical presence in the inflammatory environment in the CNS, since inhibiting their entry into the CNS compartment with anti-CD317 mAb ameliorated clinical EAE, but did not eliminate these cells from the peripheral blood.

$CD11c^+$ cells from $CD11c.Cre^{+/-}ITGA4^{fl/fl}$ mice have a significantly reduced expression of α4-integrin. Despite this observation, $CD11c^+$ cells are merely delayed in, but not prevented from, gaining access to the CNS. Ultimately, $CD11c^+$ cells are abundantly present inside the brain and spinal cord of $CD11c.Cre^{+/-}ITGA4^{fl/fl}$ mice at EAE disease onset following active immunization. We posit that this intriguing observation may point to a redundancy in the usage of adhesion molecules in $CD11c^+$ myeloid cells in gaining access to the CNS compartment. Work by other investigators suggests that macrophages utilize CD317 as an adhesion molecule to gain access to their target tissue during inflammation (21). In our study, $CD11c^+CD88^+$ cells circulated and sequestered in the peripheral blood of $CD11c.Cre^{+/-}ITGA4^{fl/fl}$ mice, and it was only after they acquired the expression of CD317 that they gained access to the CNS. The exact role and mechanism how CD317 expression endows these cells with access to the CNS, and whether it serves directly as an alternative adhesion molecule that substitutes or complements α4-integrin, needs further study.

CD317 is constitutively expressed by many cell types, including myeloid cells and B-lymphocytes (19, 20). There are species-specific differences regarding the expression of CD317. While human plasmacytoid DC express low amounts of surface CD317, this does not similarly apply to plasmacytoid DCs in mice (31). The promoter region of CD317 contains multiple *cis*-regulatory elements for transcription factors, including STAT (32, 35). Engagement of STAT induces the expression of CD317 after exposure to type I and type II IFNs (22–24), consistent with our in vitro data, and lending support to the concept that $CD11c^+CD88^+$ cells in the blood can up-regulate CD317 during active EAE under the influence of IFN-γ. In $CD11c^+CD88^+CD317^+$ cells, STAT-1 and NF-κB expression is up-regulated compared to naïve microglia or active EAE microglia, supporting their role as proinflammatory cells during EAE. One ligand of CD317 that has been identified as the surface molecule immunoglobulin-like transcript 7 (ILT7) (36, 37), which is expressed by immature plasmacytoid DC (31). Furthermore, the adhesion of myeloid cells to endothelial cells appears to be partially mediated by CD317 on endothelial cells (21), which presumably interact with ILT7 on myeloid cells. Thus, the effects we observed on clinical EAE and the distribution of $CD11c^+CD88^+CD317^+$ cells after anti-CD317 therapy may be due to binding of anti-CD317 mAb to $CD11c^+CD88^+CD317^+$cells in blood, or to endothelial cells in the CNS, or both. Our data favor an effect of anti-CD317 on $CD11c^+CD88^+CD317^+$cells, as

the differences in the percentages of $CD11c^+$ cells and $CD11c^+CD88^+$ in the blood, brain, and spinal cord in the anti-CD317 treatment group were driven by changes in the percentages of $CD11c^+CD88^+CD317^+$ cells. It was difficult to detect $CD11c^+CD88^+CD317^+$cells in blood. These observations suggest an expression of CD317 on $CD11c^+CD88^+$ in the blood immediately prior to their egress from the blood into the CNS.

Expression of CD317 by $CD11c^+CD88^+$ cells is partially induced by IFN-γ. This was shown through in vitro culture of $CD11c^+CD88^+$ cells. This observation provides one possible explanation for the distinct clinical phenotypes observed in active EAE vs. adoptive transfer EAE in $CD11c.Cre^{+/-}ITGA4^{fl/fl}$ mice. In active EAE, the activation of $CD4^+$ T cells by myelin autoantigen and CFA results in the generation of autoreactive Th17 and Th1 cells, the latter producers of IFN-γ. Consequently, a microenvironment is created outside of the CNS that provides exposure to IFN-γ that may up-regulate CD317 on $CD11c^+$ $CD88^+$ cells in active EAE. However, the adoptive transfer of myelin-reactive $CD4^+$ T cells, which includes both Th1 and Th17 cells, provides IFN-γ signaling preferentially inside the CNS after the T cells have migrated there (27–29). Thus, in the setting of adoptive transfer EAE, $CD11c^+CD88^+$ cells lack IFN-γ outside the CNS to induce CD317. Our in vitro Boyden chamber assay data indicates that access to IFN-γ significantly increases the migratory capability of $CD11c^+CD88^+CD317^+$ cells across biological barriers.

Interestingly, our human CSF transcriptome analyses placed $ITGAX^+C5AR1^+BST2^+$ cells within a population of myeloid cells that was previously defined as CSF microglia (12, 13, 38, 39). We found that activated, but not naive murine microglia, concomitantly express CD11c, CD88, and CD317. We believe these data indicate that bone marrow-derived CNS $CD11c^+CD88^+CD317^+$ cells associated with CNS autoimmune disease resemble activated parenchymal microglia. At this point, it is unclear whether these are independent cell populations with similar phenotypes and function, or whether there is a sequential development from one to the other. Future research will focus on determining which of the murine myeloid subsets in EAE recently defined by scRNA-seq express CD317 (40).

Proinflammatory myeloid cells during the pathogenesis of EAE have been described previously. Along these lines, central roles were reported for $CCR2^+$ myeloid cells (41), tissue resident classic DC (42), microglia vs. peripherally seeded monocyte-derived DC (18), and proinflammatory $iNOS^+$ macrophages vs. antiinflammatory Arg-1^+ macrophages (42). Our observations add to the complexity of categorizing myeloid cell populations

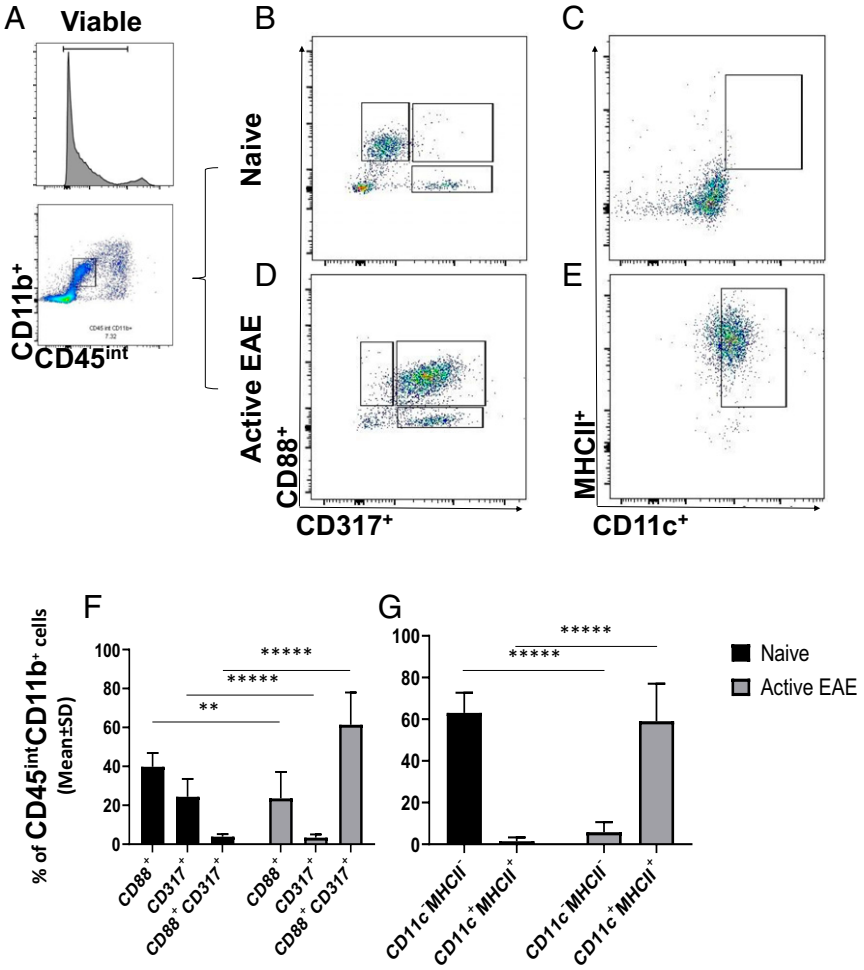

Fig. 6. Activated, but not naive microglia express CD11c, CD88, and CD317. Active EAE was induced in C57BL/6 WT mice. Brains and spinal cords were isolated and dissociated. (*A*) Microglia were defined as viable CD45 intermediate (int), $CD11b^+$ cells. (*B*) In microglia from naïve cells, these cells did not express CD88 and CD317 concomitantly. (*C*) Moreover, naïve microglia are not high expressers of MHC II and CD11c. In contrast, microglia from mice with established active EAE express high levels of (*D*) CD88 and CD317, as well as (*E*) MHC II and CD11c. The differences in the expression of (*F*) CD88, CD317, MHC II, and (*G*) CD11c were highly significant ($n = 6$ experimental animals per group; data show pooled analysis of all study cohorts; (**$P < 0.005$ or *****$P < 0.000005$).

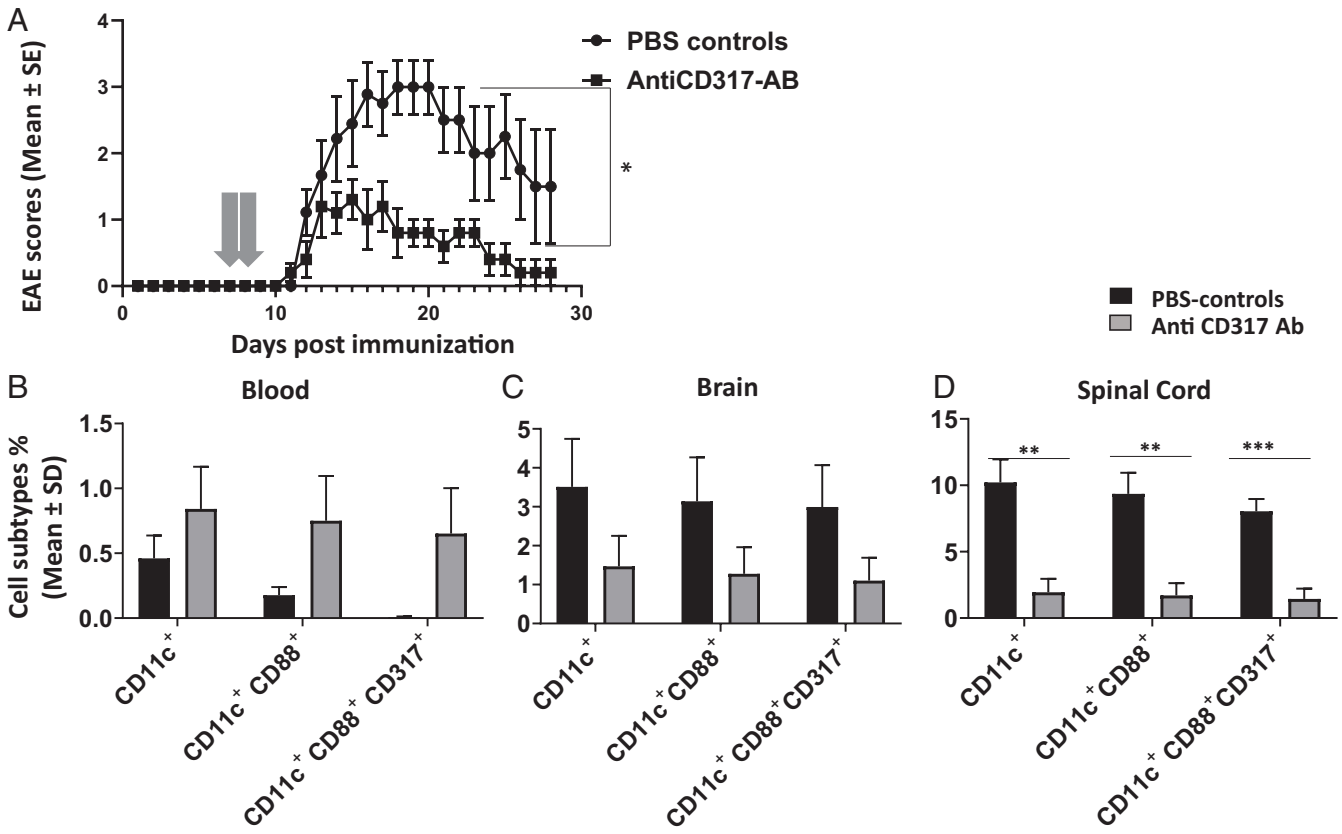

Fig. 7. Anti-CD317 treatment prevents established EAE. (*A*) EAE was actively induced in C57BL/6 WT mice. The mean ± SE of clinical EAE scores following the injection of anti-CD317 mAb in active EAE are shown ($n = 10$ experimental animals per group; data show pooled analysis from all study cohorts). There was a significant amelioration of clinical scores in the anti-CD317 mAb treatment group compared to PBS controls (*$P < 0.05$). (*B*) The mice in the anti-CD317 mAb treatment group showed a trend of sequestration of $CD11c^+$ cells, $CD11c^+CD88^+$ cells, and $CD11c^+CD88^+CD317^+$ cells in the blood however the differences were not statistically significant ($n = 4$ experimental animals per group; data show pooled analysis of all study cohorts). In the anti-CD317 mAb treatment group, $CD11c^+$ cells, $CD11c^+CD88^+$ cells, and $CD11c^+CD88^+CD317^+$ cells were less frequent in the (*C*) brain and (*D*) spinal cord. A statistically significant difference was observed in the spinal cords between the two treatment groups (**$P < 0.005$ and ***$P < 0.0005$).

into DC or monocytes/macrophages based on surface markers alone. Our results suggest that detailed morphological and functional profiling is required to provide a more profound categorization and function-based understanding of the role of these cells during different stages of EAE.

In conclusion, here we show that $CD11c^+CD88^+CD317^+$ cells appear to be critical mediators of disease in EAE that are intimately associated with the onset of disease. These cells originate from peripheral myeloid cells and their disease-propagating effects can be successfully antagonized using an mAb directed against CD317. We speculate that this pathway holds potential as a novel therapeutic option in MS.

Data Availability. All study data are included in the article and *SI Appendix*.

ACKNOWLEDGMENTS. This study was funded by Merit Review Grants federal award document number (FAIN) BX005664-01 and FAIN I01BX001674 from the US Department of Veterans Affairs, Biomedical Laboratory Research and Development (to O.S.); E.E. was supported by a Shawn Hu and Angela Zeng graduate fellowship; B.T.E. was supported by the Washington University Institute of Clinical and Translational Science Clinical and Translational Research Funding Program supported by the Foundation for Barnes-Jewish Hospital; G.F.W. was supported by the National Institute of Neurological Disorders and Stroke (Grant R01NS106289) and the National Multiple Sclerosis Society (Grant RG-1802-30253); and A.H.C. was supported in part by The Manny and Rosalyn Rosenthal and Dr. John L. Trotter Chair in Neuroimmunology of the Foundation for Barnes-Jewish Hospital. Research reported in this publication was supported by generous donations from the Lisa Novelly Fund of the John Trotter MS Center, and the Frala Osherow Fund for MS Research. Research was also supported by Washington University Institute of Clinical and Translational Sciences Grant UL1TR002345 from the National Center for Advancing Translational Sciences of the NIH. The content is solely the responsibility of the authors and does not necessarily represent the official view of the NIH.

1. R. Milo, A. D. Korczyn, N. Manouchehri, O. Stüve, The temporal and causal relationship between inflammation and neurodegeneration in multiple sclerosis. *Mult. Scler.* **26**, 876–886 (2019).
2. B. Serafini *et al*., Dendritic cells in multiple sclerosis lesions: Maturation stage, myelin uptake, and interaction with proliferating T cells. *J. Neuropathol. Exp. Neurol.* **65**, 124–141 (2006).
3. M. Greter *et al*., Dendritic cells permit immune invasion of the CNS in an animal model of multiple sclerosis. *Nat. Med.* **11**, 328–334 (2005).
4. M. del Pilar Martin *et al*., Decrease in the numbers of dendritic cells and CD4+ T cells in cerebral perivascular spaces due to natalizumab. *Arch. Neurol.* **65**, 1596–1603 (2008).
5. L. M. Scott, G. V. Priestley, T. Papayannopoulou, Deletion of alpha4 integrins from adult hematopoietic cells reveals roles in homeostasis, regeneration, and homing. *Mol. Cell. Biol.* **23**, 9349–9360 (2003).
6. M. L. Caton, M. R. Smith-Raska, B. Reizis, Notch-RBP-J signaling controls the homeostasis of CD8- dendritic cells in the spleen. *J. Exp. Med.* **204**, 1653–1664 (2007).
7. N. Manouchehri *et al*., Limitations of cell-lineage-specific non-dynamic gene recombination in CD11c.Cre$^+$ITGA4$^{fl/fl}$ mice. *J. Neuroimmunol.* **344**, 577245 (2020).
8. R. Z. Hussain *et al*., Defining standard enzymatic dissociation methods for individual brains and spinal cords in EAE. *Neurol. Neuroimmunol. Neuroinflamm.* **5**, e437 (2018).
9. R. Z. Hussain *et al*., TLR3 agonism re-establishes CNS immune competence during α4-integrin deficiency. *Ann. Clin. Transl. Neurol.* **5**, 1543–1561 (2018).
10. R. Z. Hussain *et al*., α4-integrin deficiency in B cells does not affect disease in a T-cell-mediated EAE disease model. *Neurol. Neuroimmunol. Neuroinflamm.* **6**, e563 (2019).
11. A. Albini *et al*., A rapid in vitro assay for quantitating the invasive potential of tumor cells. *Cancer Res.* **47**, 3239–3245 (1987).

12. E. Esaulova *et al*., Single-cell RNA-seq analysis of human CSF microglia and myeloid cells in neuroinflammation. *Neurol. Neuroimmunol. Neuroinflamm.* **7**, e732 (2020).
13. S. F. Farhadian *et al*., Single-cell RNA sequencing reveals microglia-like cells in cerebrospinal fluid during virologically suppressed HIV. *JCI Insight* **3**, e121718 (2018).
14. L. S. Davis, N. Oppenheimer-Marks, J. L. Bednarczyk, B. W. McIntyre, P. E. Lipsky, Fibronectin promotes proliferation of naive and memory T cells by signaling through both the VLA-4 and VLA-5 integrin molecules. *J. Immunol.* **145**, 785–793 (1990).
15. Y. Shimizu, G. A. van Seventer, K. J. Horgan, S. Shaw, Costimulation of proliferative responses of resting CD4+ T cells by the interaction of VLA-4 and VLA-5 with fibronectin or VLA-6 with laminin. *J. Immunol.* **145**, 59–67 (1990).
16. I. L. King, T. L. Dickendesher, B. M. Segal, Circulating Ly-6C+ myeloid precursors migrate to the CNS and play a pathogenic role during autoimmune demyelinating disease. *Blood* **113**, 3190–3197 (2009).
17. P. Deshpande, I. L. King, B. M. Segal, Cutting edge: CNS CD11c+ cells from mice with encephalomyelitis polarize Th17 cells and support CD25+CD4+ T cell-mediated immunosuppression, suggesting dual roles in the disease process. *J. Immunol.* **178**, 6695–6699 (2007).
18. D. A. Giles, P. C. Duncker, N. M. Wilkinson, J. M. Washnock-Schmid, B. M. Segal, CNS-resident classical DCs play a critical role in CNS autoimmune disease. *J. Clin. Invest.* **128**, 5322–5334 (2018).
19. G. Palma *et al*., Plasmacytoids dendritic cells are a therapeutic target in anticancer immunity. *Biochim. Biophys. Acta* **1826**, 407–414 (2012).
20. Y. M. El-Sherbiny *et al*., B cell tetherin: A flow cytometric cell-specific assay for response to type I interferon predicts clinical features and flares in systemic lupus erythematosus. *Arthritis Rheumatol.* **72**, 769–779 (2019).
21. H. Yoo, S.-H. Park, S.-K. Ye, M. Kim, IFN-γ-induced BST2 mediates monocyte adhesion to human endothelial cells. *Cell. Immunol.* **267**, 23–29 (2011).
22. S. J. Neil, T. Zang, P. D. Bieniasz, Tetherin inhibits retrovirus release and is antagonized by HIV-1 Vpu. *Nature* **451**, 425–430 (2008).
23. N. Van Damme *et al*., The interferon-induced protein BST-2 restricts HIV-1 release and is downregulated from the cell surface by the viral Vpu protein. *Cell Host Microbe* **3**, 245–252 (2008).
24. A. L. Blasius *et al*., Bone marrow stromal cell antigen 2 is a specific marker of type I IFN-producing cells in the naive mouse, but a promiscuous cell surface antigen following IFN stimulation. *J. Immunol.* **177**, 3260–3265 (2006).
25. M. Merad, P. Sathe, J. Helft, J. Miller, A. Mortha, The dendritic cell lineage: Ontogeny and function of dendritic cells and their subsets in the steady state and the inflamed setting. *Annu. Rev. Immunol.* **31**, 563–604 (2013).
26. G. Arellano, P. A. Ottum, L. I. Reyes, P. I. Burgos, R. Naves, Stage-specific role of interferon-gamma in experimental autoimmune encephalomyelitis and multiple sclerosis. *Front. Immunol.* **6**, 492 (2015).
27. S. S. Zamvil *et al*., Encephalitogenic T cell clones specific for myelin basic protein. An unusual bias in antigen recognition. *J. Exp. Med.* **162**, 2107–2124 (1985).
28. M. K. Racke, Experimental autoimmune encephalomyelitis (EAE). *Curr. Protoc. Neurosci.*, chap. 9, Unit 9.7 (2001).
29. P. D. Cravens *et al*., Lymph node-derived donor encephalitogenic CD4+ T cells in C57BL/6 mice adoptive transfer experimental autoimmune encephalomyelitis highly express GM-CSF and T-bet. *J. Neuroinflammation* **8**, 73 (2011).
30. R. Sankowski *et al*., Mapping microglia states in the human brain through the integration of high-dimensional techniques. *Nat. Neurosci.* **22**, 2098–2110 (2019).
31. W. Cao *et al*., Regulation of TLR7/9 responses in plasmacytoid dendritic cells by BST2 and ILT7 receptor interaction. *J. Exp. Med.* **206**, 1603–1614 (2009).
32. T. Ohtomo *et al*., Molecular cloning and characterization of a surface antigen preferentially overexpressed on multiple myeloma cells. *Biochem. Biophys. Res. Commun.* **258**, 583–591 (1999).
33. E. L. Gautier *et al*.; Immunological Genome Consortium, Gene-expression profiles and transcriptional regulatory pathways that underlie the identity and diversity of mouse tissue macrophages. *Nat. Immunol.* **13**, 1118–1128 (2012).
34. O. Butovsky *et al*., Identification of a unique TGF-β-dependent molecular and functional signature in microglia. *Nat. Neurosci.* **17**, 131–143 (2014).
35. Y. Ge *et al*., Differential gene expression, GATA1 target genes, and the chemotherapy sensitivity of Down syndrome megakaryocytic leukemia. *Blood* **107**, 1570–1581 (2006).
36. T. L. Chapman, A. P. Heikeman, P. J. Bjorkman, The inhibitory receptor LIR-1 uses a common binding interaction to recognize class I MHC molecules and the viral homolog UL18. *Immunity* **11**, 603–613 (1999).
37. M. Shiroishi *et al*., Human inhibitory receptors Ig-like transcript 2 (ILT2) and ILT4 compete with CD8 for MHC class I binding and bind preferentially to HLA-G. *Proc. Natl. Acad. Sci. U.S.A.* **100**, 8856–8861 (2003).
38. E. Beltrán *et al*., Early adaptive immune activation detected in monozygotic twins with prodromal multiple sclerosis. *J. Clin. Invest.* **129**, 4758–4768 (2019).
39. D. Schafflick *et al*., Integrated single cell analysis of blood and cerebrospinal fluid leukocytes in multiple sclerosis. *Nat. Commun.* **11**, 247 (2020).
40. A. Giladi *et al*., Cxcl10+ monocytes define a pathogenic subset in the central nervous system during autoimmune neuroinflammation. *Nat. Immunol.* **21**, 962 (2020).
41. B.D. Clarkson *et al*., CCR2-dependent dendritic cell accumulation in the central nervous system during early effector experimental autoimmune encephalomyelitis is essential for effector T cell restimulation in situ and disease progression. *J. Immunol.* **194**, 531–541 (2015).
42. D. A. Giles *et al*., Myeloid cell plasticity in the evolution of central nervous system autoimmunity. *Ann. Neurol.* **83**, 131–141 (2018).